Supporting Information

Selective Propargylic C(sp^3)–H Activation of Methyl-Substituted Alkynes Versus [2+2]-Cycloaddition at a Titanium Imido Template

Malte Fischer,[ac+*] Manfred Manßen,[bc+*] Marc Schmidtmann,[c] Thorsten Klüner,[c*] and Rüdiger Beckhaus[c*]

[+] equal contribution

[a] Dr. M. Fischer
Inorganic Chemistry Laboratory, Department of Chemistry, University of Oxford, South Parks Road, Oxford, OX1 3QR
E-mail: malte.fischer@chem.ox.ac.uk

[b] Dr. M. Manßen
The Department of Chemistry, The University of British Columbia, 2036 Main Mall, Vancouver, BC, Canada
E-mail: manssen@chem.ubc.ca

[c] Dr. Malte Fischer, Dr. Manfred Manßen, Dr. M. Schmidtmann, Prof. Dr. T. Klüner, Prof. Dr. R. Beckhaus
Institut für Chemie, Fakultät für Mathematik und Naturwissenschaften, Carl von Ossietzky Universität Oldenburg, Postfach 2503, 26111 Oldenburg, Germany
E-mail: ruediger.beckhaus@uni-oldenburg.de

Table of Contents

General Considerations

All reactions were carried out under an inert atmosphere of argon or nitrogen with rigorous exclusion of oxygen and moisture using standard glovebox and Schlenk techniques unless stated otherwise. The glass equipment was stored in an oven at 120 °C and evacuated prior to use. Solvents and liquid educts were dried according to standard procedures. Solvents were distilled over Na/K alloy and benzophenone or CaH_2 under nitrogen atmosphere. Solid materials were stored and weighted in a glove box or dried under high vacuum prior to use. The titanium imide **1b** (in equilibrium with the titanium amide **1a**), and the titanaazacyclobutene **I** were synthesized according to literature procedures.[S1]

NMR spectra were recorded on a Bruker Avance 300, Bruker Avance 500, and Bruker Avance III 500 spectrometer. ^{1}H NMR spectra were referend to the residual solvent resonance as internal standard (benzene-d_6 (C_6D_6): $\delta^{1}H(C_6D_5H)$ = 7.16 ppm), and $^{13}C\{^{1}H\}$ spectra by using the central line of the solvent signal (benzene-d_6 (C_6D_6): $\delta^{13}C\{^{1}H\}(C_6D_6)$ = 128.06 ppm). The given chemical shifts of ^{15}N NMR spectra resulting out of $^{15}N/^{1}H$ HMQC NMR experiments with nitromethane as external standard (δ = 378.9 vs. NH_3).

Infrared spectra were measured on a Bruker Tensor 27 spectrometer with a MKII Reflection Golden Gate Single Diamond ATR system.

Elemental analyses were carried out on a EuroEA 3000 Elemental Analyzer.

Melting points were determined using a “Mel-Temp” by Laboratory Devices, Cambridge, U.K..

Thin-layer chromatography was performed using commercially available Alugram SIL/G UV254 sheets with fluorescent indicator (254 nm) from Macherey Nagel. Silica gel from Grace (particle size 40-63 µm) was used for column chromatography.

Synthesis and characterization of compounds:

Synthesis of 2a:

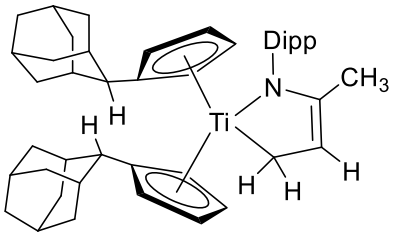

Complex **1b** (in equilibrium with **1a**) (0.540 g, 0.905 mmol) was dissolved in 15 mL of *n*-hexane. 2-Butyne (0.1 mL, 0.905 mmol) was added to the solution. The reaction mixture was stirred for 120 h at room temperature. All volatile components were removed under vacuum to yield complex **2a** as red-brown solid.

Crystals suitable for single-crystal X-ray diffraction were obtained by slow evaporation of an *n*-hexane solution of **2a**.

Yield: 0.386 g (0.675 mmol, 75%).

Melting point: 126-128 °C (dec.).

IR (ATR): $\tilde{\nu}$ = 2960, 2899, 2847, 1528, 1466, 1449, 1435, 1381, 1361, 1320, 1240, 1191, 1099, 1062, 1035, 955, 934, 881, 859, 802, 764, 730, 682, 664, 638 cm^{-1}.

^{1}H NMR (500 MHz, C_6D_6, 305 K): δ = 0.81-0.83 (m, 1H, $TiCH_2$), 1.11 (d, $^{3}J_{H,H}$ = 6.9 Hz, 3H, $CH_{3,\,iPr}$), 1.17 (d, $^{3}J_{H,H}$ = 6.7 Hz, 3H, $CH_{3,iPr}$), 1.19 (d, $^{3}J_{H,H}$ = 6.7 Hz, 3H, $CH_{3,iPr}$), 1.32 (d, $^{3}J_{H,H}$ = 6.9 Hz, 3H, $CH_{3,iPr}$), 1.45-2.16 (m, 28H, CH_{Ad}/$CH_{2,Ad}$), 1.69 (s, 3H, $HC{=}C_qC\mathit{H}_3$), 1.96 (m, 1H, CH_{iPr})*, 2.36-2.38 (m, 1H, $TiCH_2$), 2.47 (s, 1H, CH_{exo}), 2.89 (s, 1H, CH_{exo}), 3.74 (hept, $^{3}J_{H,H}$ = 6.7 Hz, 1H, CH_{iPr}), 4.93-4.95 (m, 1H, C_5H_4), 5.08-5.11 (m, 2H, $\mathit{H}C{=}C_qCH_3$, C_5H_4), 5.29-5.30 (m, 1H, C_5H_4), 5.42-5.43 (m, 1H, C_5H_4), 5.48-5.49 (m, 1H, C_5H_4), 5.56-5.57 (m, 2H, 2×C_5H_4), 5.92-5.93 (m, 1H, C_5H_4), 7.03-7.05 (m, 1H, C_6H_3), 7.11-7.12 (m, 2H, C_6H_3) ppm.

^{13}C{^{1}H} NMR (126 MHz, C_6D_6, 305 K): δ = 20.6 ($HC{=}C_q\underline{C}H_3$), 23.8 (CH_{iPr}), 24.8 ($CH_{3,iPr}$), 24.9 ($CH_{3,iPr}$), 25.6 ($CH_{3,iPr}$), 26.5 ($CH_{3,iPr}$), 27.0 (CH_{iPr}), 28.2 (CH_{Ad}), 28.37 (CH_{Ad}), 28.43 (CH_{Ad}), 28.5 (CH_{Ad}), 32.0 (CH_{Ad}), 32.1 ($CH_{2,Ad}$), 32.2 ($CH_{2,Ad}$), 32.4 ($CH_{2,Ad}$), 32.6 ($CH_{2,Ad}$), 32.8 (CH_{Ad}), 33.0 (CH_{Ad}), 33.7 (CH_{Ad}), 38.3 ($CH_{2,Ad}$), 38.4 ($CH_{2,Ad}$), 39.15 ($CH_{2,Ad}$), 39.17 ($CH_{2,Ad}$), 39.3 (2×$CH_{2,Ad}$), 43.9 (2×CH_{exo}), 64.9 ($TiCH_2$), 96.7 (C_5H_4), 102.7 (C_5H_4), 104.2 (C_5H_4), 106.3 (C_5H_4), 107.2 (C_5H_4), 108.7 (C_5H_4), 109.2 (C_5H_4), 110.9 (C_5H_4), 111.6 ($H\underline{C}{=}C_qCH_3$), 118.5 ($C_{q,ipso}$), 123.7 (C_6H_3), 124.0 (C_6H_3), 125.5 (C_6H_3), 128.1 ($C_{q,ipso}$)**, 140.6 ($HC{=}\underline{C}_qCH_3$), 142.7 ($C_{q,6}H_3$), 143.7 ($C_{q,6}H_3$), 149.2 ($C_{q,6}H_3$) ppm.

* = overlap with CH_{Ad}/$CH_{2,Ad}$ signals

** = overlap with C_6D_6 signal

^{15}N/^{1}H HMBC NMR (51 MHz, C_6D_6, 305 K): δ = 266.3 ppm.

EA: Anal. calcd. for $C_{46}H_{61}NTi$: C, 81.75; H, 9.10; N, 2.07; Found: C, 81.57; H, 9.55; N, 2.28.

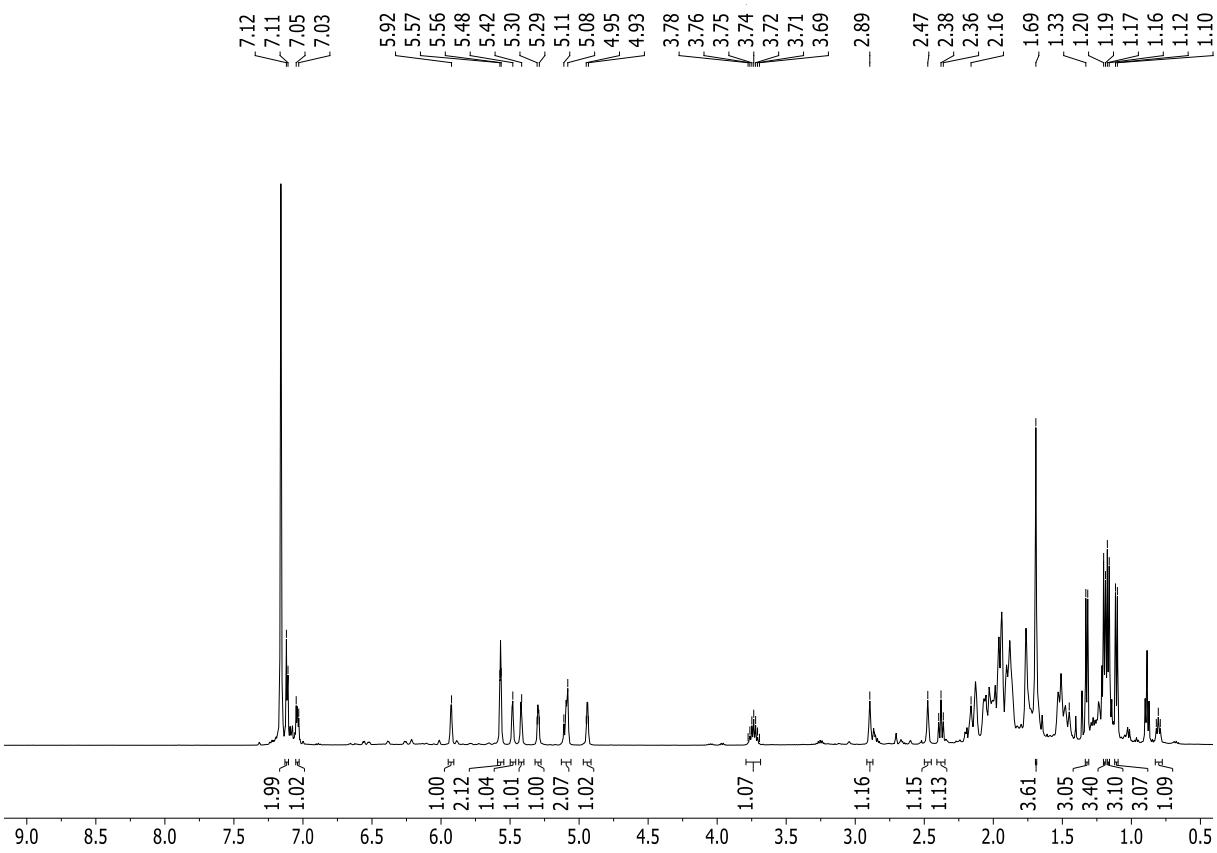

Figure S1: ^{1}H NMR spectrum of **2a** (500 MHz, C_6D_6, rt).

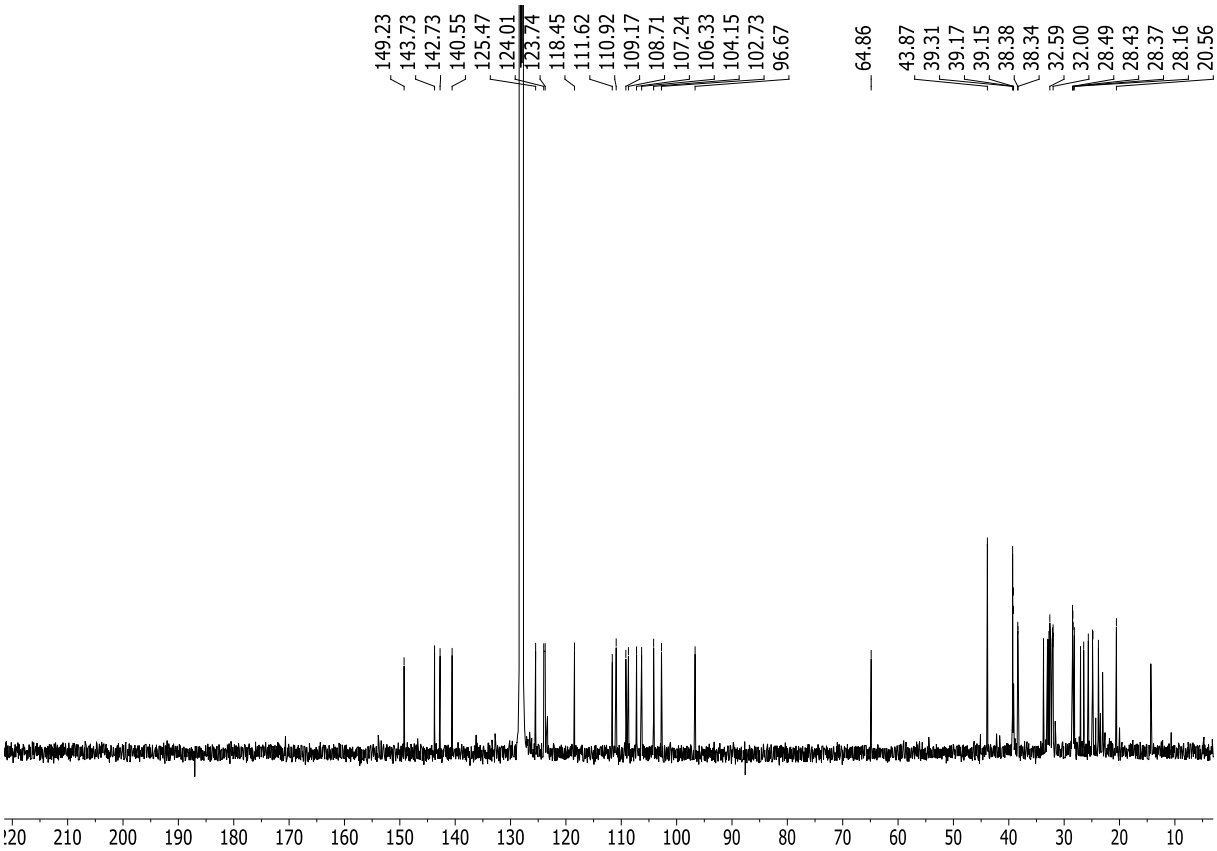

Figure S2: $^{13}C\{^{1}H\}$ NMR spectrum of **2a** (126 MHz, C_6D_6, rt).

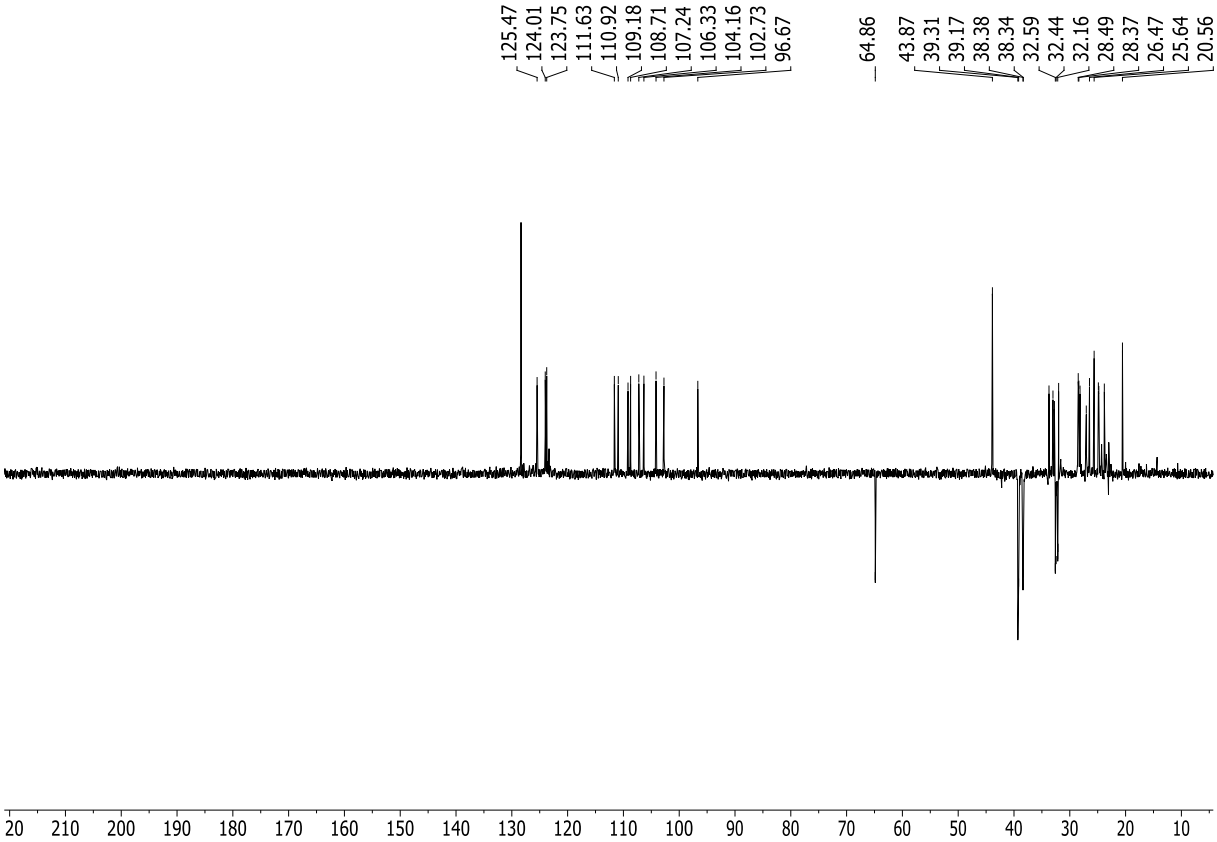

Figure S3: $^{13}C\{^{1}H\}$ DEPT 135 NMR spectrum of **2a** (126 MHz, C_6D_6, rt).

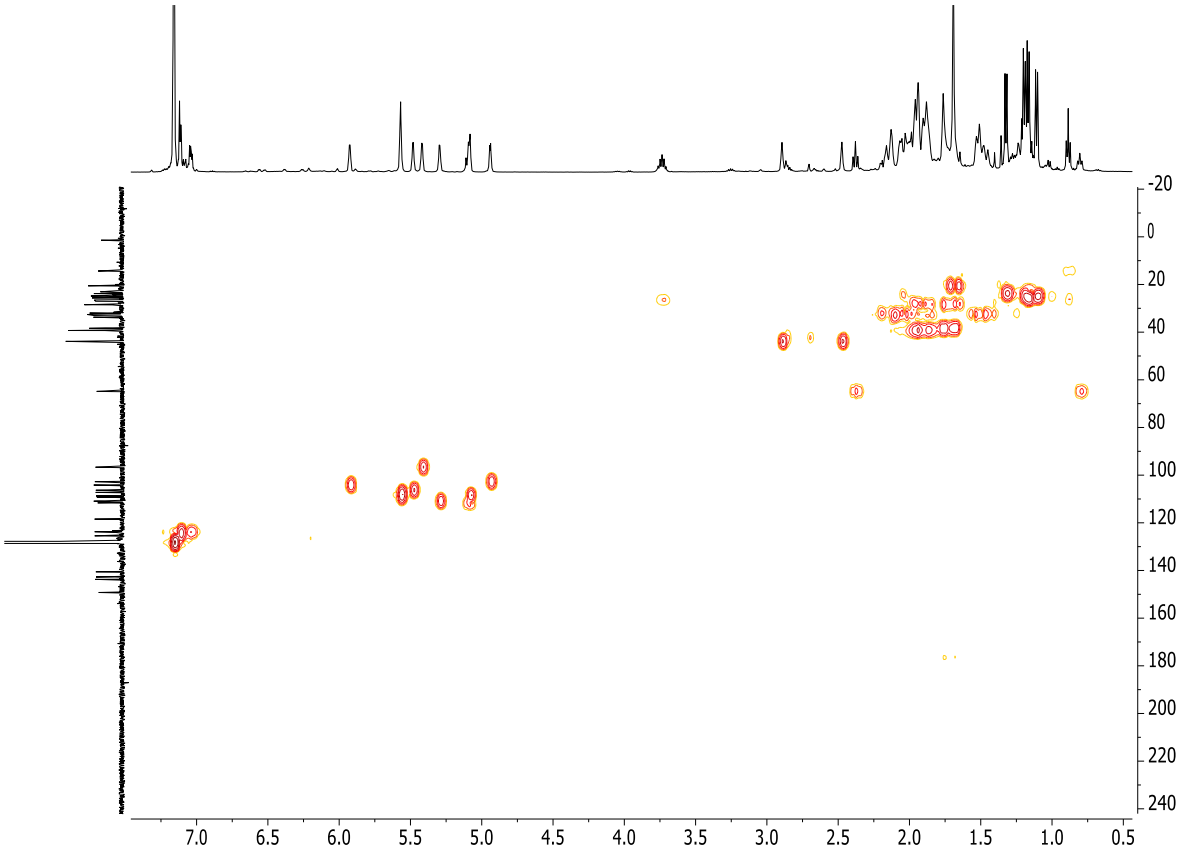

Figure S4: $^{1}H/^{13}C\{^{1}H\}$ HSQC NMR spectrum of **2a** (C_6D_6, rt).

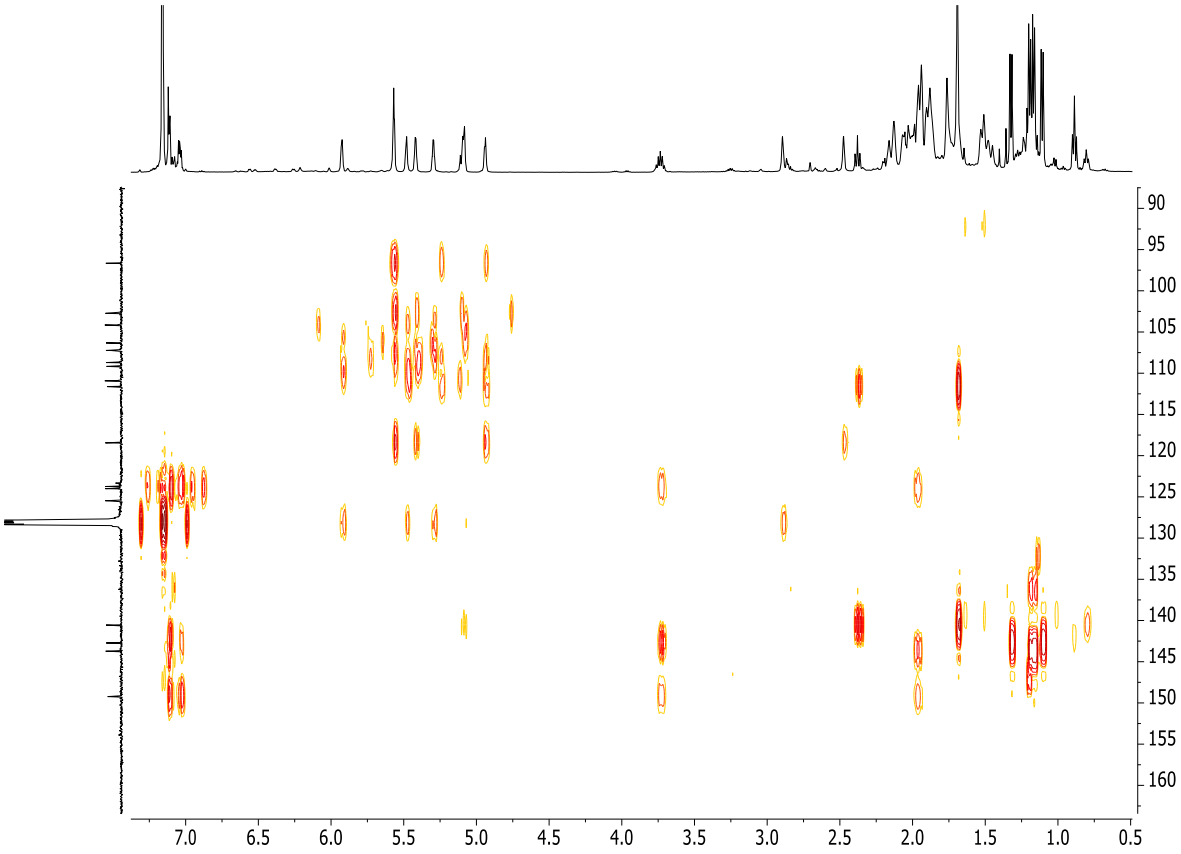

Figure S5: $^{1}H/^{13}C\{^{1}H\}$ HMBC NMR spectrum of **2a** (C_6D_6, rt).

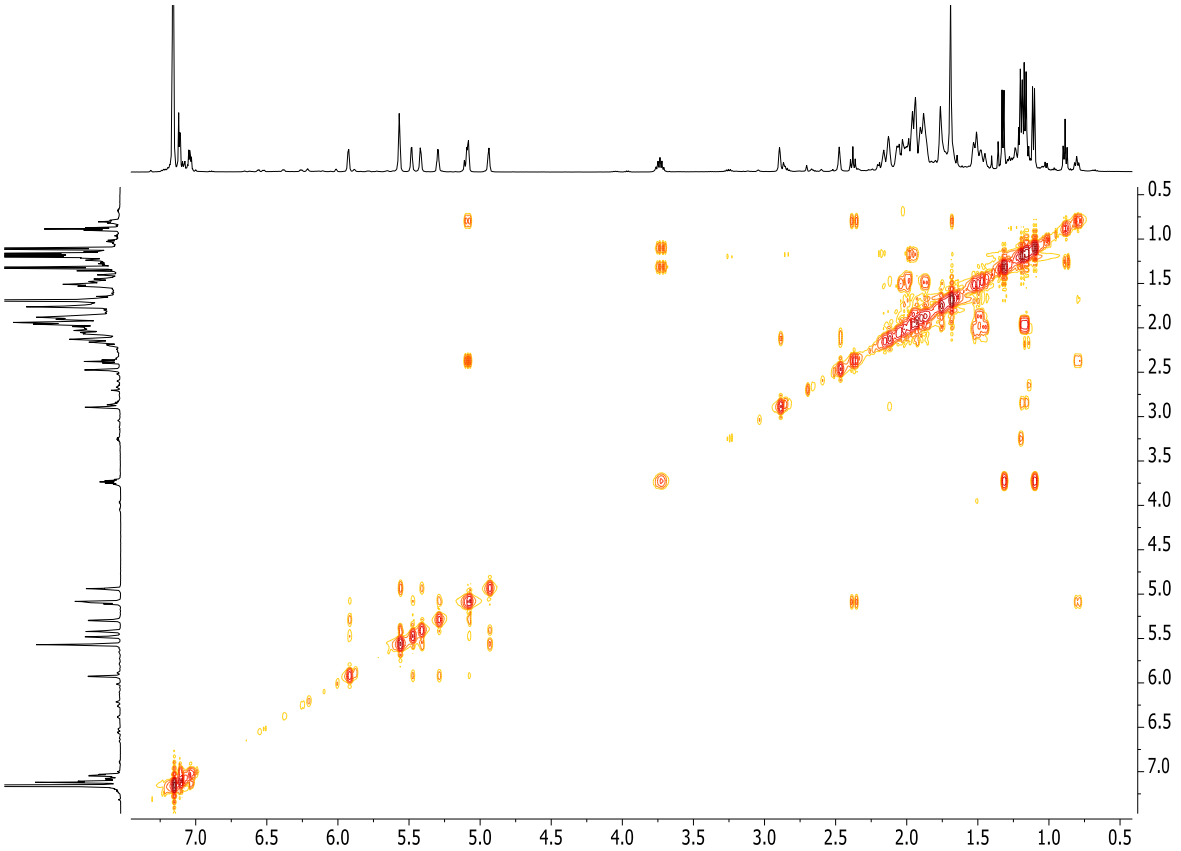

Figure S6: $^{1}H/^{1}H$ COSY NMR spectrum of **2a** (C_6D_6, rt).

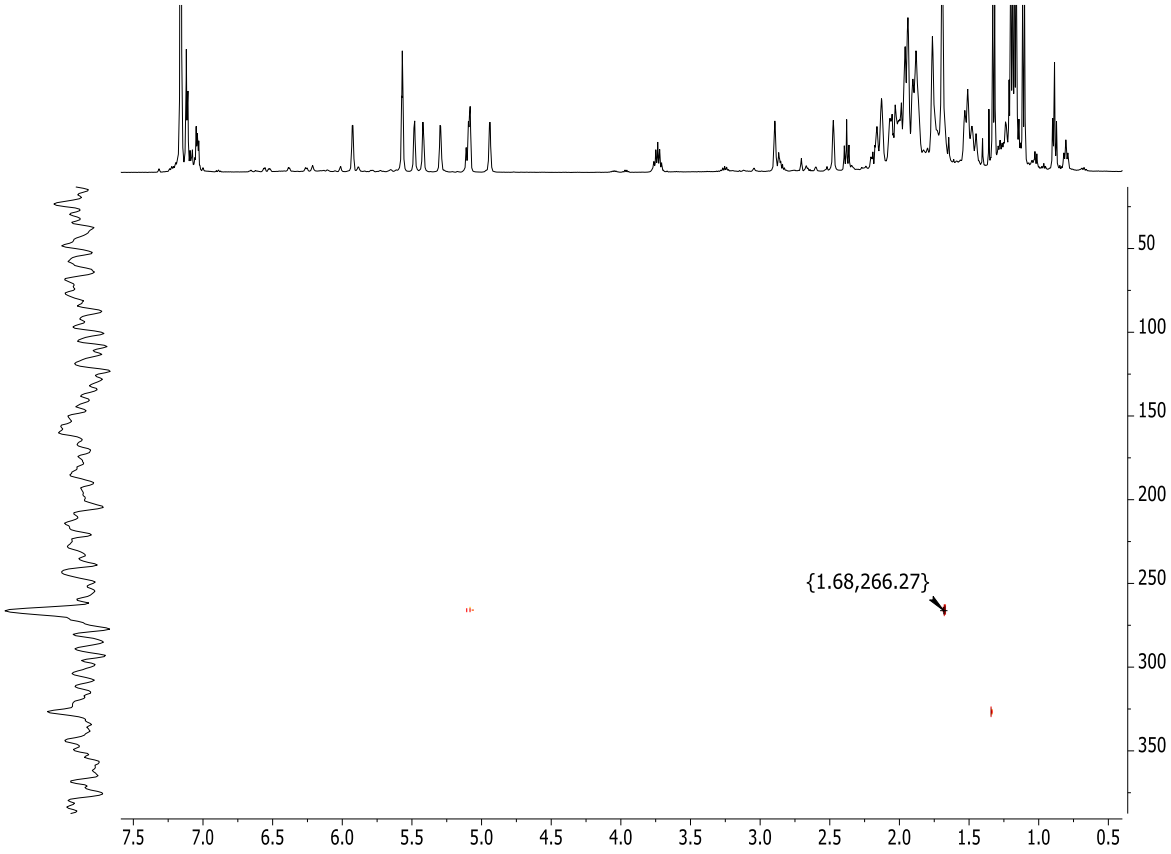

Figure S7: $^{15}N/^{1}H$ HMBC NMR spectrum of **2a** (51 MHz, C_6D_6, rt).

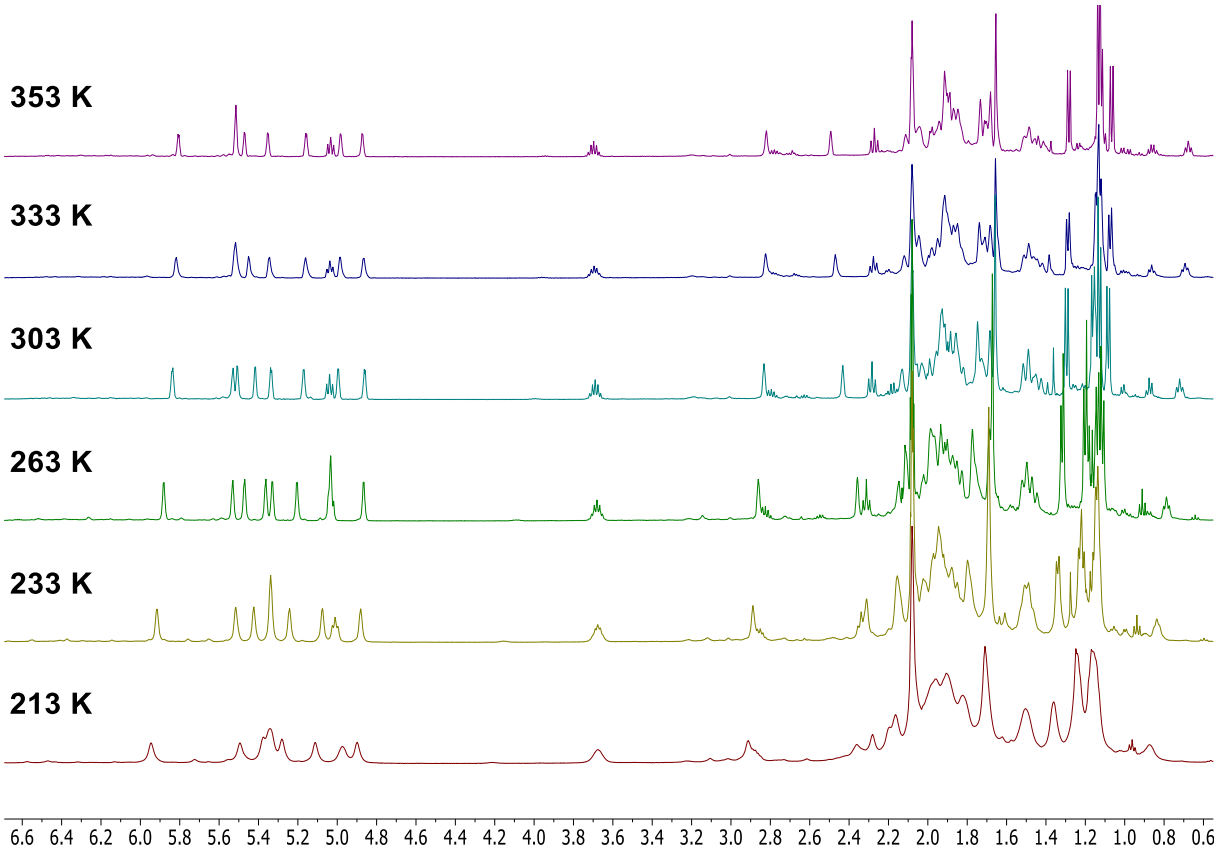

Figure S8: VT ^{1}H NMR spectrum of **2a** (500 MHz, C_6D_6, 213 - 353 K).

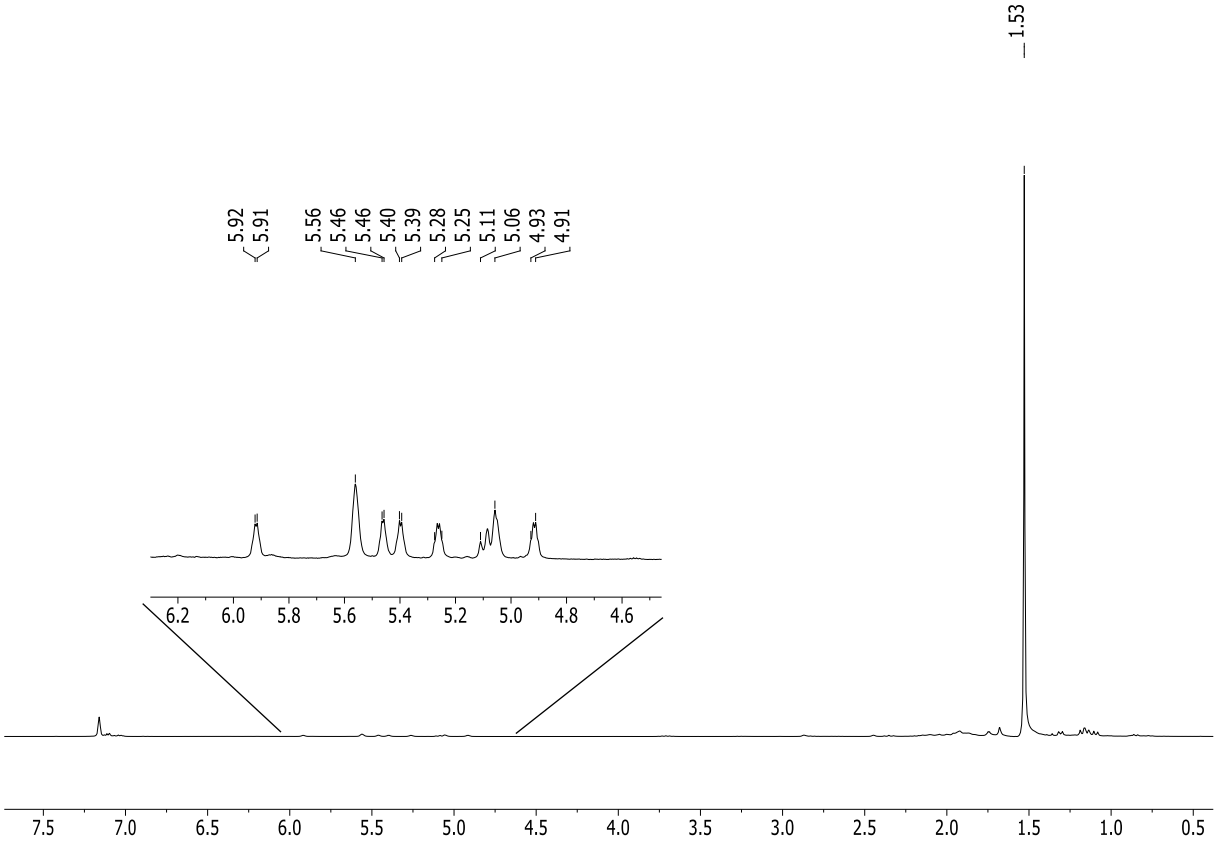

Figure S9: ^{1}H NMR spectrum of the reaction of **2a** with excess 2-butyne (500 MHz, C_6D_6, rt); 1.53 ppm: 2-butyne.

Synthesis of 2b:

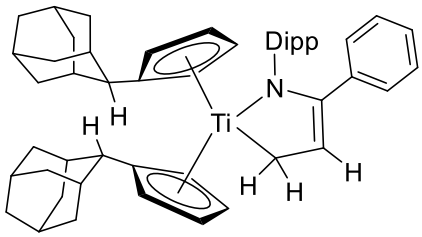

Titanaazacyclobutene **I** (0.040 g, 0.054 mmol) was dissolved in 0.6 mL of C_6D_6 and transferred to a Young NMR tube. The probe was slowly heated and regularly monitored by ^{1}H NMR spectroscopy (Figure S17). After one week no further reaction progress could be observed and the multinuclear and 2D NMR analyses were subsequently performed. The evaluation of the data verified that the titanamonoazadiene **2b** was obtained. The formation of **2b** is accompanied by some side product formations.

Crystals suitable for single crystal X-ray diffraction of **2b** were obtained by slow evaporation of the C_6D_6 solution.

^{1}H NMR (500 MHz, C_6D_6, 305 K): δ = 0.94 (d, $^3J_{H,H}$ = 6.6 Hz, 3H, $CH_{3,\ iPr}$), 0.98-1.00 (m, 1H, $TiCH_2$)*, 1.15 (d, $^3J_{H,H}$ = 6.8 Hz, 3H, $CH_{3,\ iPr}$), 1.38 (d, $^3J_{H,H}$ = 6.8 Hz, 3H, $CH_{3,\ iPr}$), 1.46 (d, $^3J_{H,H}$ = 6.6 Hz, 3H, $CH_{3,\ iPr}$), 1.48-2.23 (m, 30H, CH_{Ad}/$CH_{2,Ad}$, CH_{iPr}), 2.42 (s, 1H, CH_{exo}), 2.55-2.58 (m, 1H, $TiCH_2$), 2.92 (s, 1H, CH_{exo}), 4.01 (hept, $^3J_{H,H}$ = 6.7 Hz, 1H, CH_{iPr}), 5.13-5.14 (m, 1H, C_5H_4), 5.19-5.20 (m, 1H, C_5H_4), 5.39-5.41 (m, 1H, C_5H_4), 5.53-5.58 (m, 4H, C_5H_4), 5.66-5.69 (m, 1H, *H*C=C_qPh), 5.99-6.00 (m, 1H, C_5H_4), 6.86-6.88 (m, 1H, CH_{Aryl}), 6.91-6.94 (m, 1H, CH_{Aryl}), 6.97-7.01 (m, 1H, CH_{Aryl}), 7.04-7.07 (m, 2H, CH_{Aryl}), 7.11-7.13 (m, 1H, CH_{Aryl}), 7.46-7.48 (m, 2H, CH_{Aryl}) ppm.

* = assigned by ^{1}H/^{13}C HMSC NMR spectroscopy

^{13}C{^{1}H} NMR (126 MHz, C_6D_6, 305 K): δ = 25.2 ($CH_{3,iPr}$), 25.4 ($CH_{3,iPr}$), 25.5 ($CH_{3,iPr}$), 25.6 ($CH_{3,iPr}$), 26.8 (CH), 27.2 (CH), 28.1 (CH), 28.3 (CH), 28.4 (CH), 28.5 (CH), 32.0 (CH), 32.02 ($CH_{2,Ad}$), 32.03 ($CH_{2,Ad}$), 32.4 ($CH_{2,Ad}$), 32.57 ($CH_{2,Ad}$), 32.62 (CH), 33.1 (CH), 33.7 (CH), 38.29 ($CH_{2,Ad}$), 39.1 ($CH_{2,Ad}$), 39.2 ($CH_{2,Ad}$), 39.27 ($CH_{2,Ad}$), 39.33 ($CH_{2,Ad}$), 40.2 ($CH_{2,Ad}$), 43.7 (CH_{exo}), 43.9 (CH_{exo}), 67.4 ($TiCH_2$), 97.5 (C_5H_4), 103.6 (C_5H_4), 105.3 (C_5H_4), 107.1 (C_5H_4), 107.5 (C_5H_4), 109.2 (C_5H_4), 109.6 (C_5H_4), 112.7 (H<u>C</u>=C_qPh), 113.3 (C_5H_4), 118.2 ($C_{q,ipso}$), 124.0 (CH_{Aryl}), 124.3 (CH_{Aryl}), 125.1 (CH_{Aryl}), 127.4 (CH_{Aryl}), 128.0 (2×CH_{Aryl})**, 128.9 (2×CH_{Aryl}), 129.5 ($C_{q,ipso}$), 138.7 (HC=<u>C</u>$_q$Ph), 142.5 ($C_{q,Aryl}$), 143.3 ($C_{q,Aryl}$), 143.7 ($C_{q,Aryl}$), 150.6 ($C_{q,Aryl}$) ppm.

* = assigned by ^{1}H/^{13}C HMSC NMR spectroscopy

** = overlap with C_6D_6 signal

^{15}N/^{1}H HMBC NMR (51 MHz, C_6D_6, 305 K): δ = 256.0 ppm.

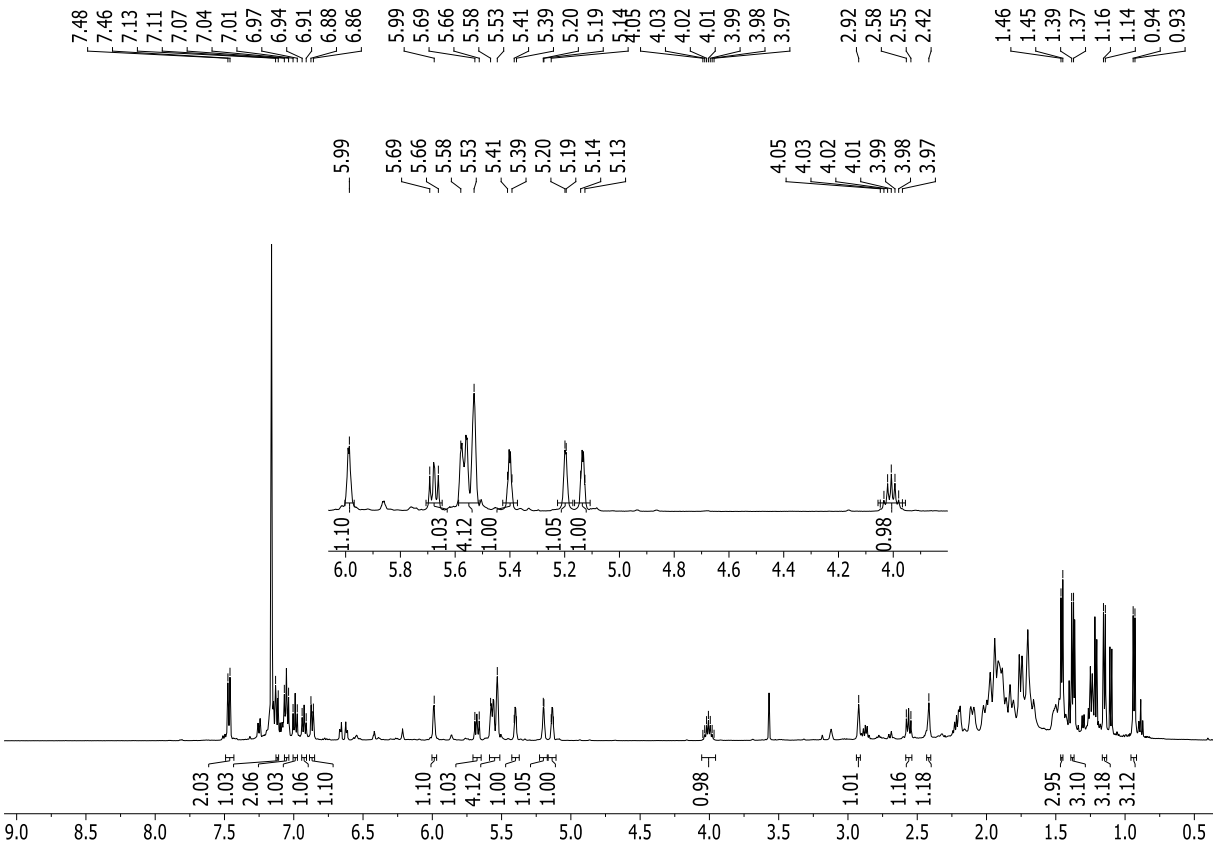

Figure S10: ^{1}H NMR spectrum of **2b** (500 MHz, C_6D_6, rt).

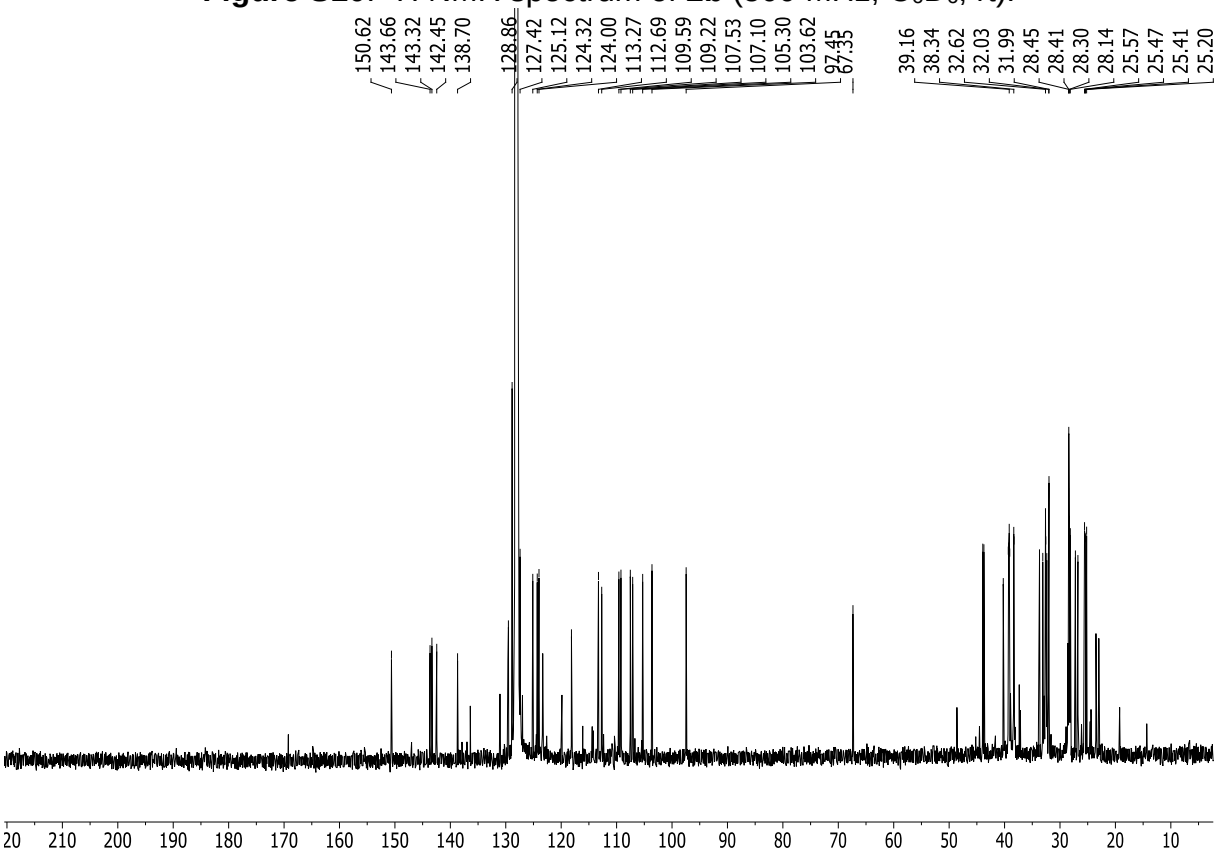

Figure S11: ^{13}C{^{1}H} NMR spectrum of **2b** (126 MHz, C_6D_6, rt).

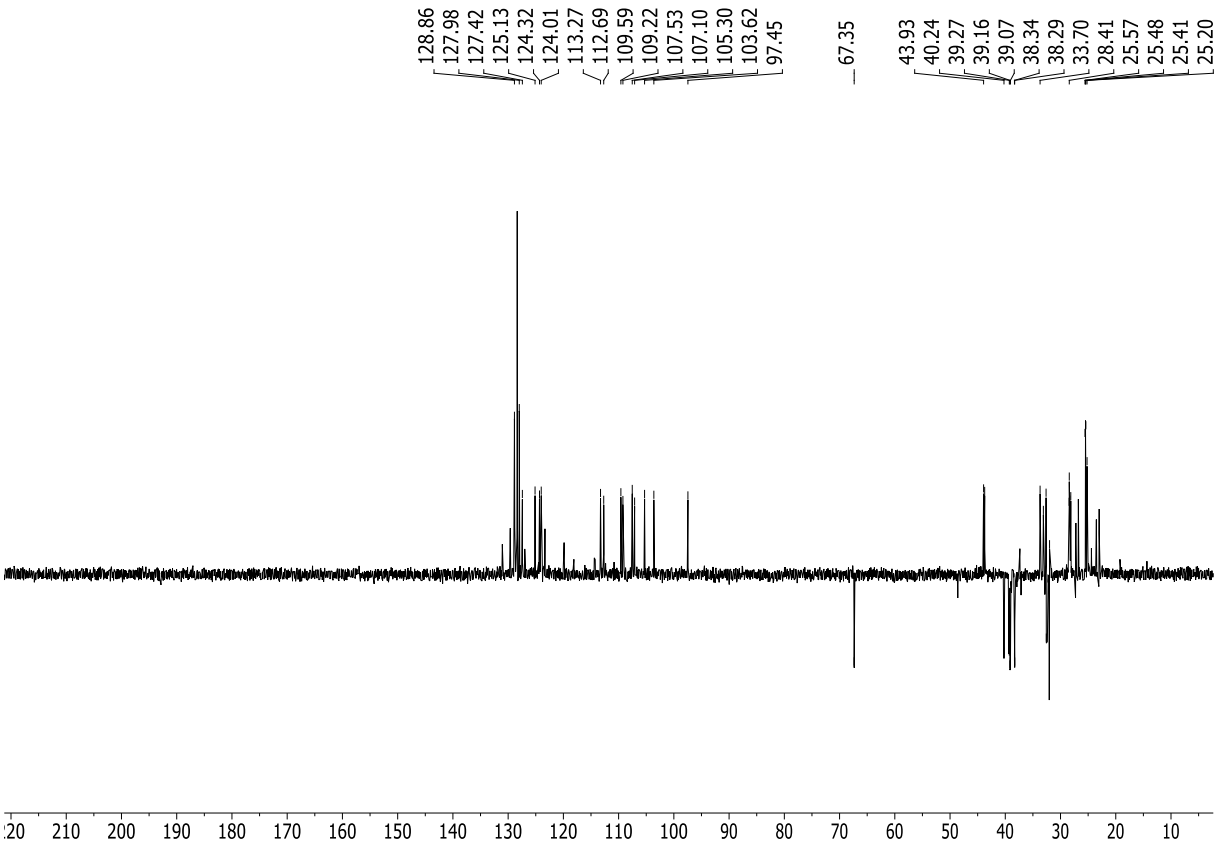

Figure S12: $^{13}C\{^{1}H\}$ DEPT 135 NMR spectrum of **2b** (126 MHz, C_6D_6, rt).

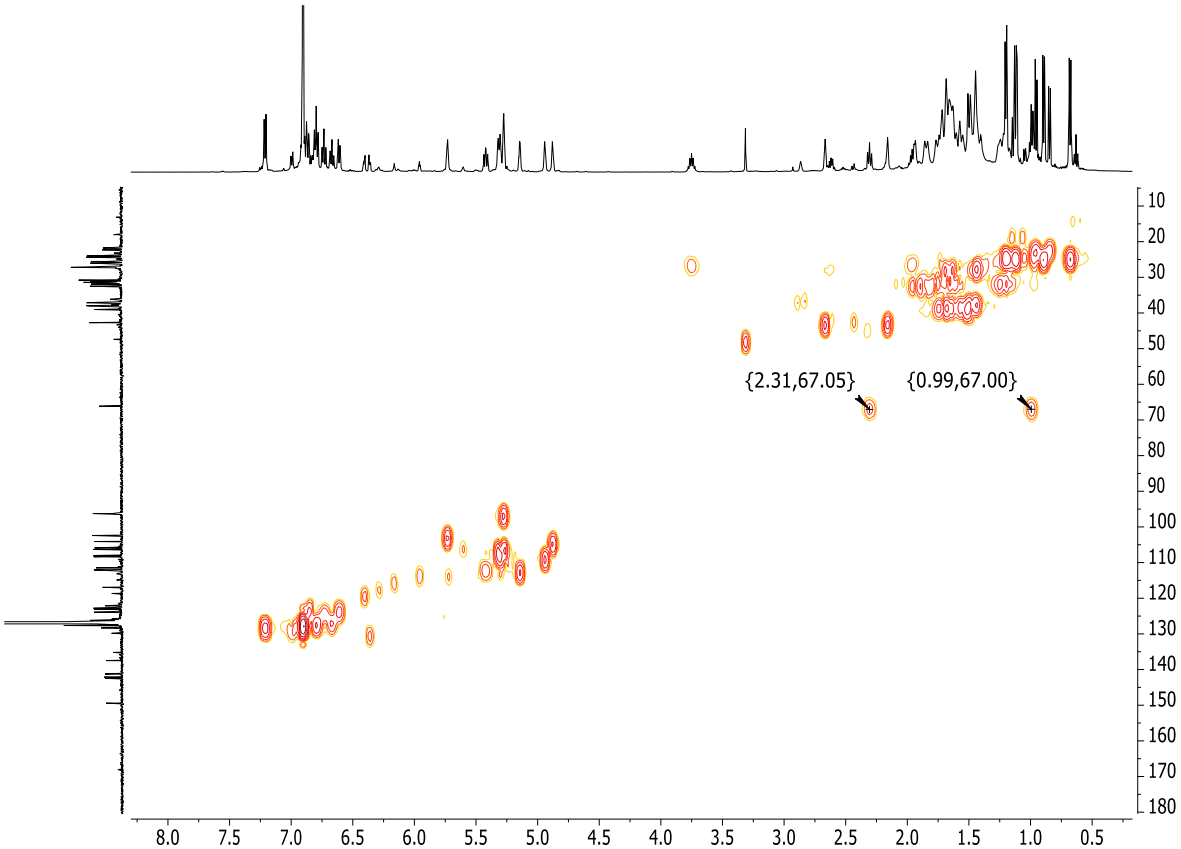

Figure S13: $^{1}H/^{13}C\{^{1}H\}$ HSQC NMR spectrum of **2b** (C_6D_6, rt).

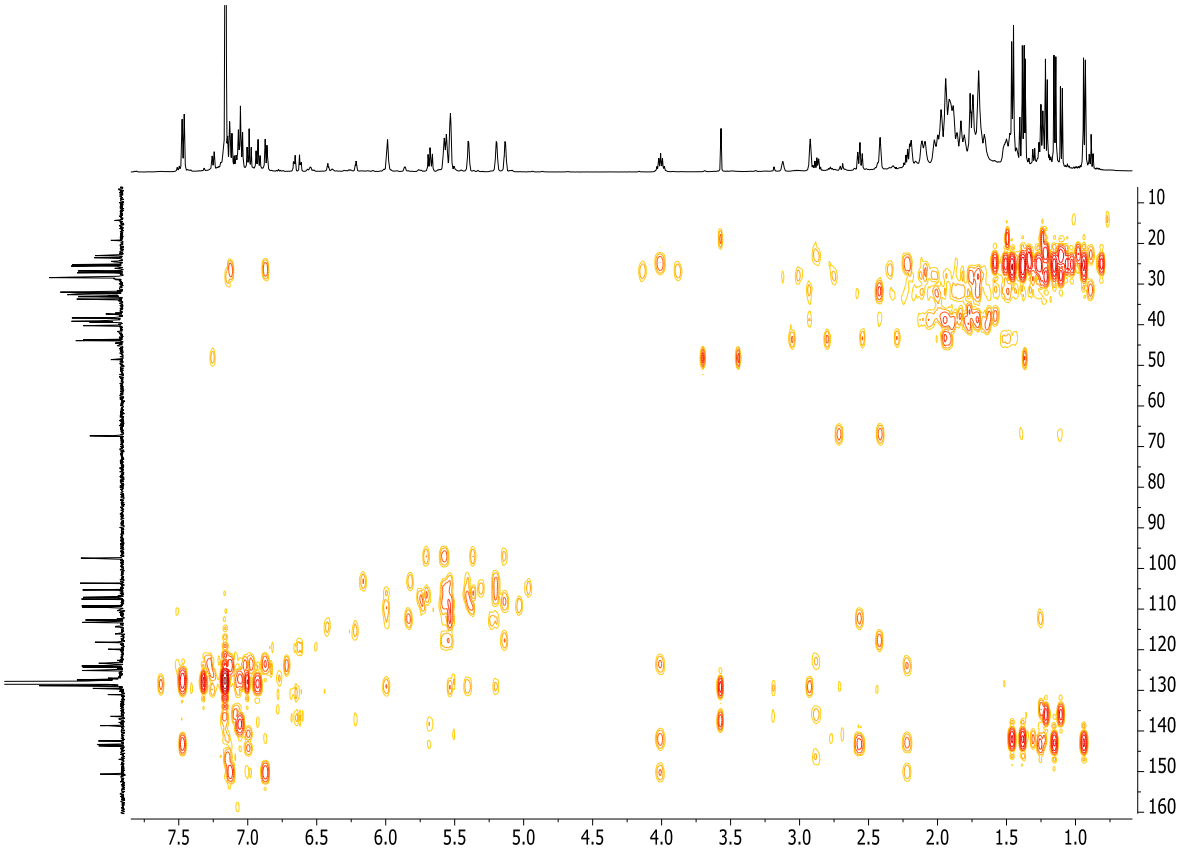

Figure S14: $^{1}H/^{13}C\{^{1}H\}$ HMBC NMR spectrum of **2b** (C_6D_6, rt).

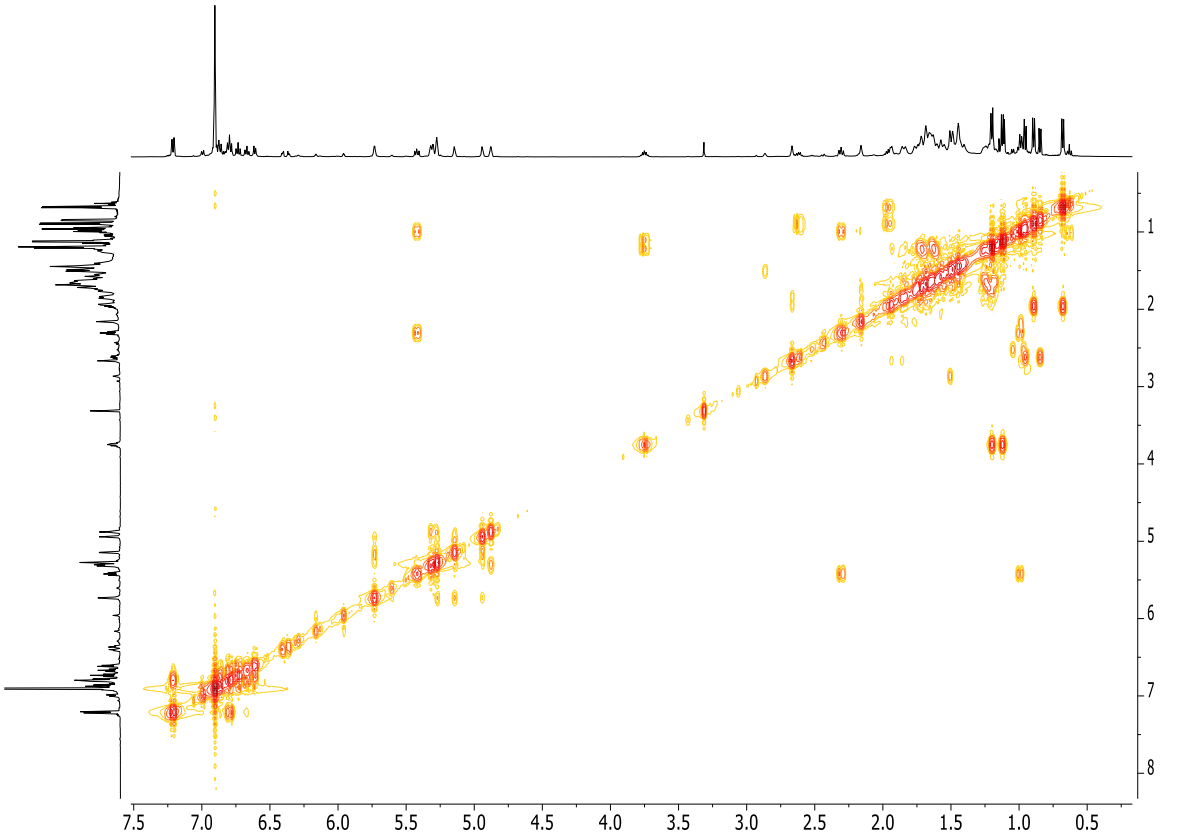

Figure S15: $^{1}H/^{1}H$ COSY NMR spectrum of **2b** (C_6D_6, rt).

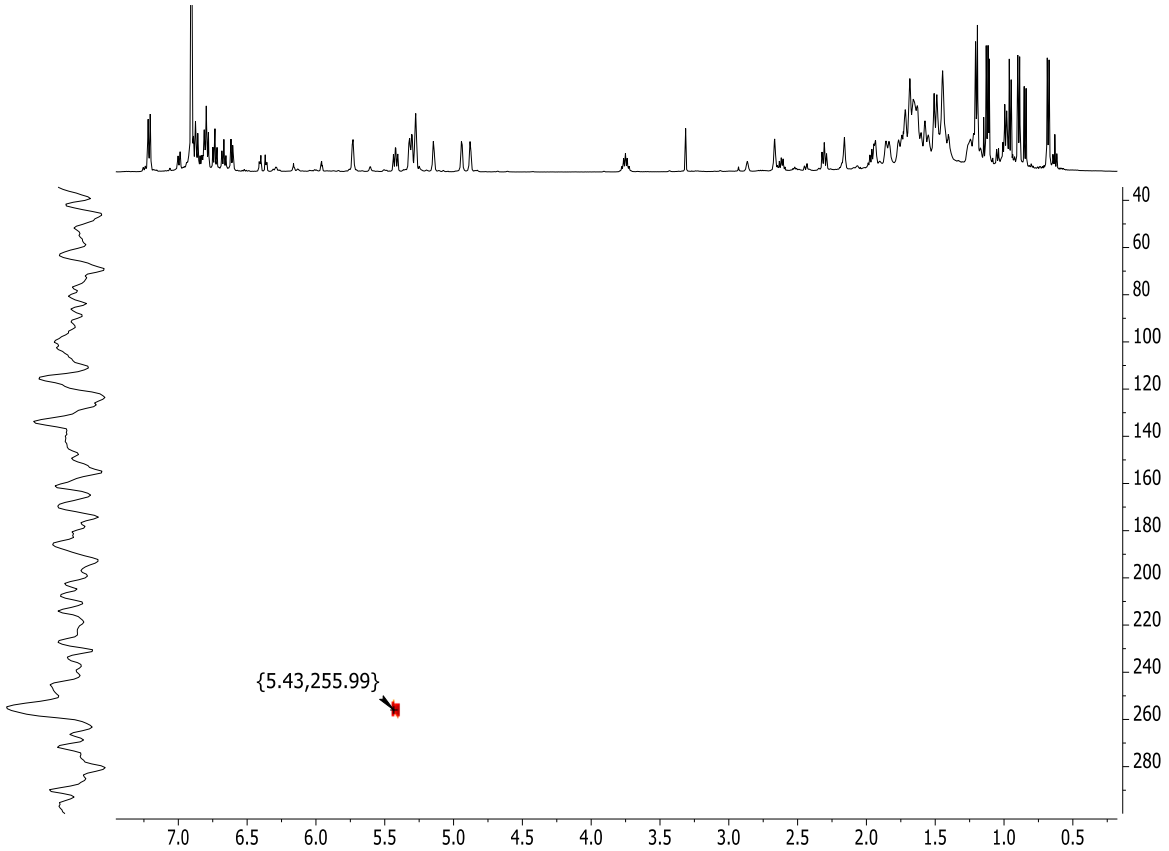

Figure S16: $^{15}N/^{1}H$ HMBC NMR spectrum of **2b** (51 MHz, C_6D_6, rt).

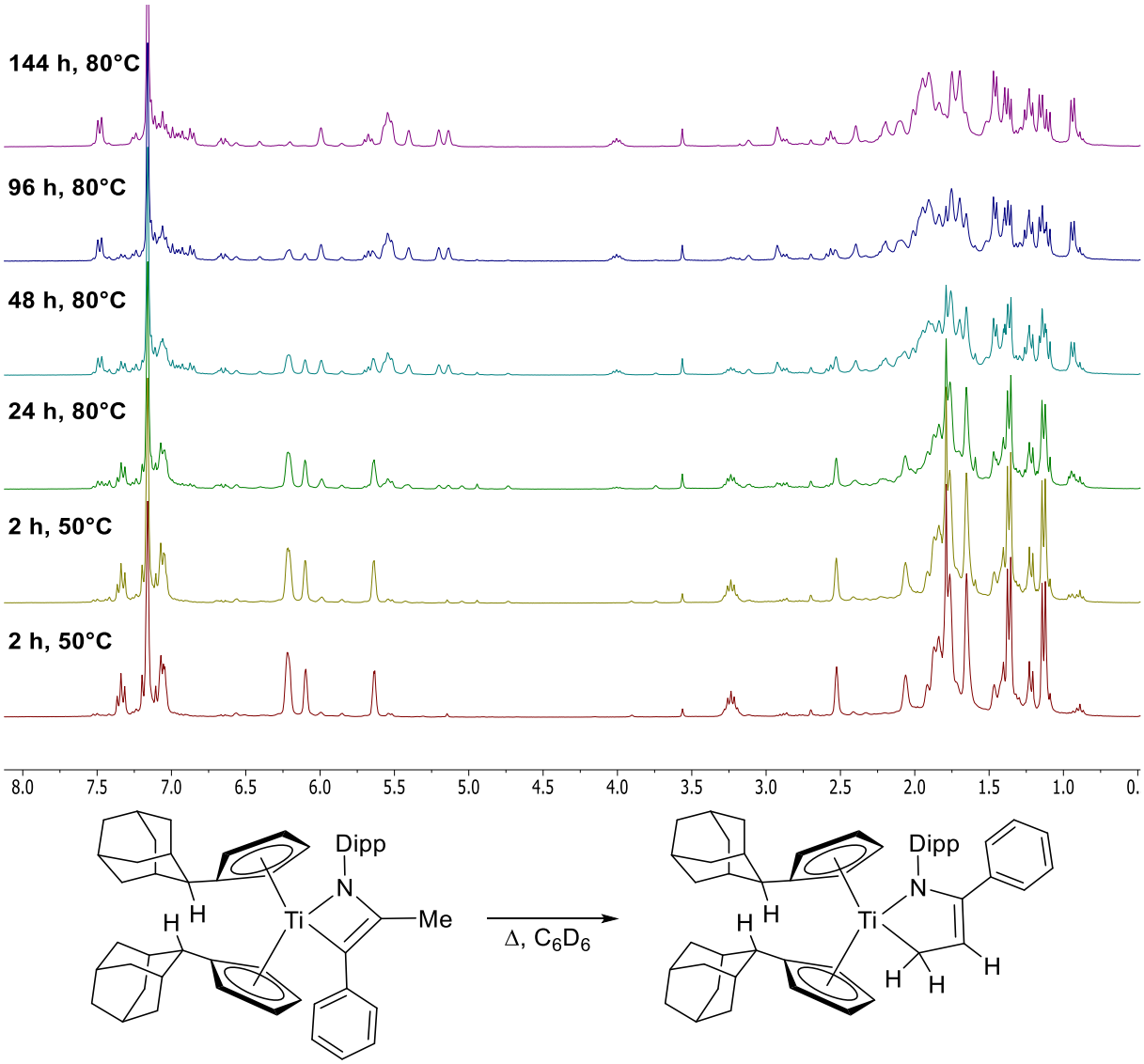

Figure S17: Monitoring of the reaction progress via ^{1}H NMR spectroscopy (500 MHz, C_6D_6, rt).

Crystallographic Data:

Single crystal X-ray data for **2a** were measured on a Bruker AXS Apex II diffractometer (graphite monochromator, Mo-Kα radiation, λ = 0.71073 Å, Kappa 4-circle goniometer, Apex II CCD detector).

Single crystal X-ray data for **2b** were measured on a Bruker AXS D8 Venture diffractometer (multilayer optics, Mo-Kα radiation with λ = 0.71073 Å, Kappa 4-circle goniometer, Photon III C14 CPAD detector).

Single crystal X-ray data for **I** were measured on a Bruker AXS D8 Venture diffractometer (multilayer optics, Cu-Kα radiation with λ = 1.54178 Å, Kappa 4-circle goniometer, Photon III C14 CPAD detector).

Empirical absorption corrections using equivalent reflections were performed with the program SADABS[S2]. The structures were solved with the program SHELXS[S3] and refined with SHELXL[S4] using the OLEX2[S5] GUI. All non H atoms were refined using anisotropic atomic displacement parameters, H atoms bonded to C were located in the difference Fourier map and placed on idealized geometric positions with idealized atomic displacement parameters using the riding model, H atoms of the CH_2 groups bonded to Ti were refined freely.

The crystal size of **I** was extremely small resulting in poor data resolution and refinement statistics. Accordingly, the resolution (alert B) results from the low scattering power of the crystal. In **2b** there are two reflections whose measured intensities differ slightly from the calculated ones. The deviations is just above the arbitrary limit set by the IUCR and there is no physical reason (e.g. partially masked by the beam stop) to remove these reflections from the data set.

The crystallographic data can be obtained free of charge from https://www.ccdc.cam.ac.uk/structures/ quoting the CCDC numbers 2070445-2070447.

Table S1: Crystal Structure Data for Compounds **2a**, **2b**, and **I**.

	2a	**I**	**2b**
CCDC	2070446	2070445	2070447
empirical formula	$C_{46}H_{61}NTi$	$C_{51}H_{63}NTi$	$C_{51}H_{63}NTi$
fw	675.85	737.92	737.92
colour	dark red	red	green red
Habit	block	needle	plate
cryst dimens, mm	0.40 x 0.30 x 0.20	0.08 x 0.02 x 0.01	0.13 x 0.075 x 0.035
cryst syst	monoclinic	monoclinic	monoclinic
space group	$P2_1/c$	$P2_1/c$	$P2_1/c$
a, Å	14.6868(8)	19.3982(6)	18.7684(9)
b, Å	11.3121(6)	19.9869(7)	15.8524(7)
c, Å	22.0238(12)	10.3954(4)	27.8285(13)
α, deg	90	90	90
β, deg	91.0155(16)	104.314(2)	109.9782(18)
γ, deg	90	90	90
V, Å^3	3658.4(3)	3905.3(2)	7959.8(6)
Z	4	4	4
D_{caclcd}, g cm^{-3}	1.227	1.255	1.232
μ, mm^{-1}	0.268	2.120	0.252
T, K	100(2)	100(2)	100(2)
θ range, deg	1.653 – 34.971	2.351 – 58.925	1.493 – 30.033
no. of rflns collected	193658	71245	372823
no. of indep rflns	16067	5606	23312
(R(int))	0.0468	0.1157	0.0725
no. of rflns with I>2σ(I)	13309	4334	19424
abs cor	semi-empirical	semi-empirical	semi-empirical
max, min transmission	1.0000 and 0.9239	1.0000 and 0.9226	1.0000 and 0.9508
final R indices	R1 = 0.0380	R1 = 0.0429	R1 = 0.0394
[I>2σ(I)]	wR2 = 0.0998	wR2 = 0.0946	wR2 = 0.0921
R indices (all data)	R1 = 0.0501 wR2 = 0.1082	R1 = 0.0642 wR2 = 0.1045	R1 = 0.0520 wR2 = 0.0986
GOF on F²	1.041	1.054	1.006
largest diff peak / hole (e.Å^{-3})	0.958 /-0.403	0.264 /-0.339	0.399 /-0.453

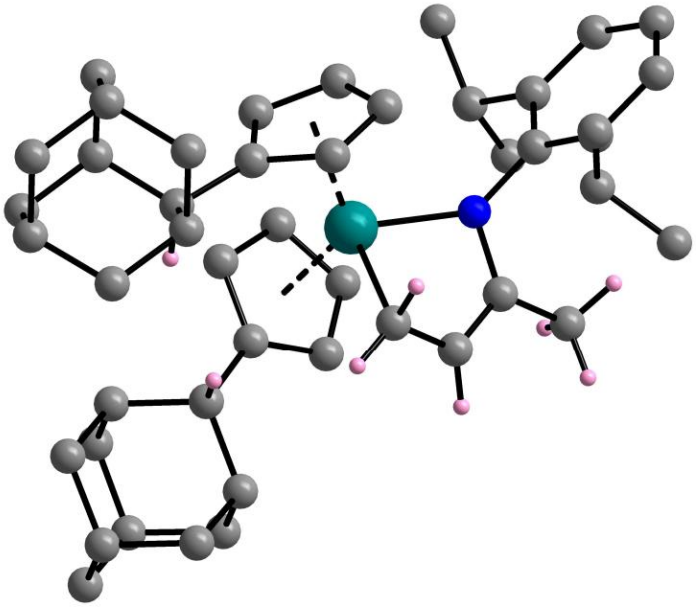

Figure S18: Molecular structure of **2a**.

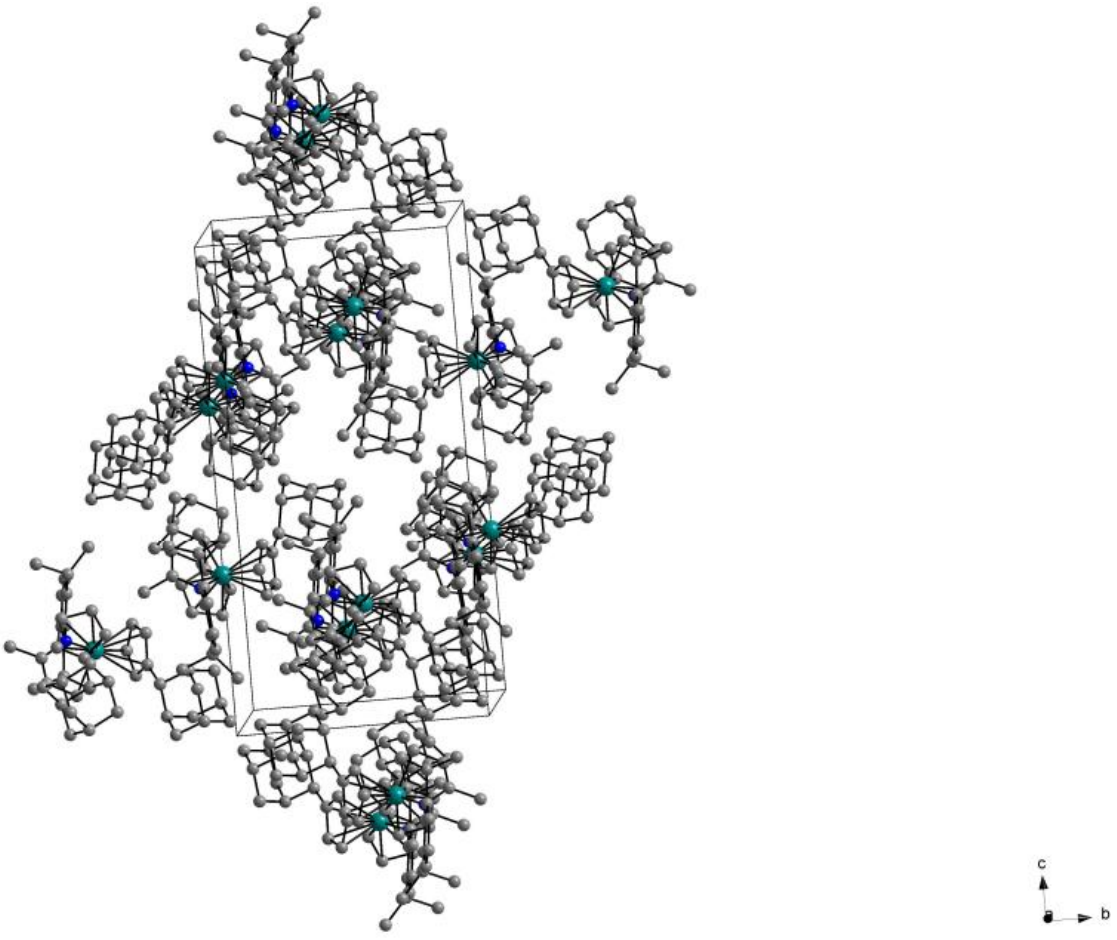

Figure S19: View along the *a* axis showing the packing of molecules in the crystal structure of complex **2a**. Hydrogen atoms have been omitted for clarity.

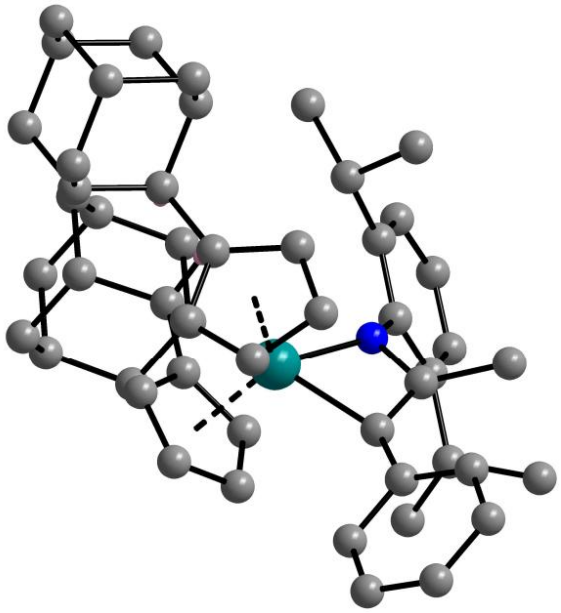

Figure S20: Molecular structure of **I**.

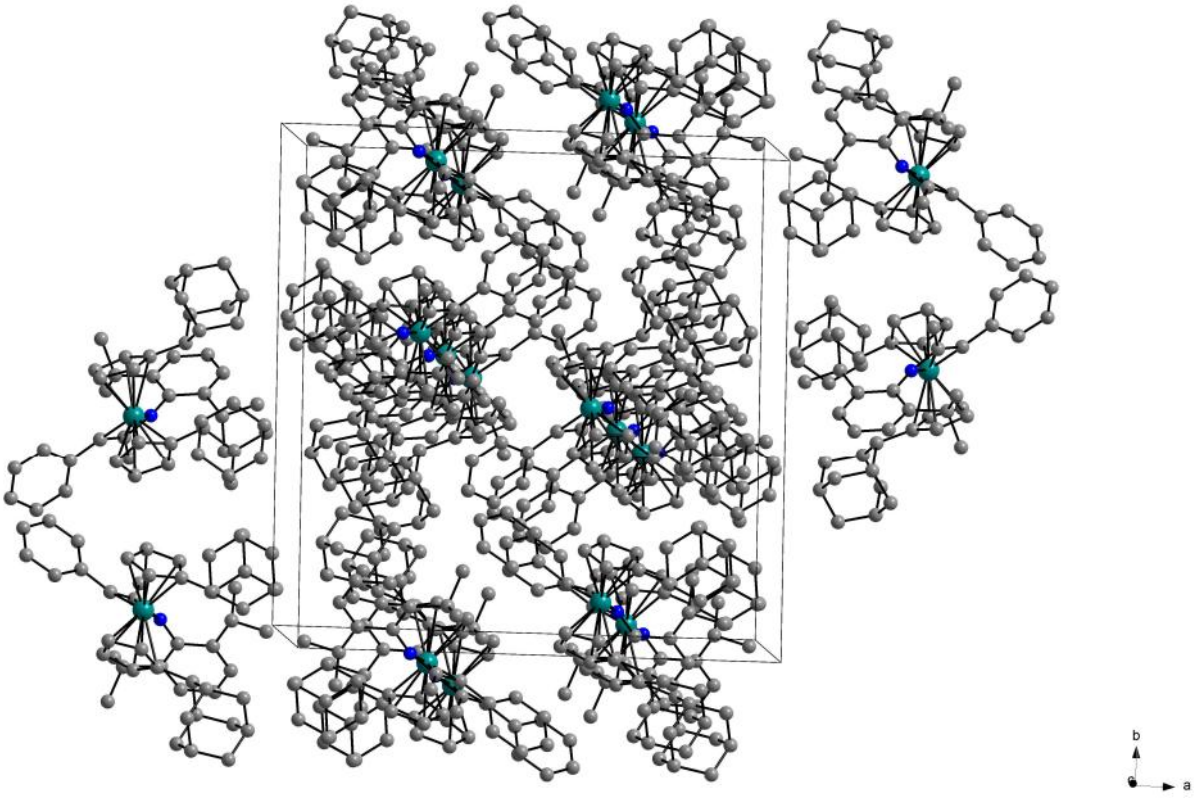

Figure S21: View along the *c* axis showing the packing of molecules in the crystal structure of complex **I**. Hydrogen atoms have been omitted for clarity.

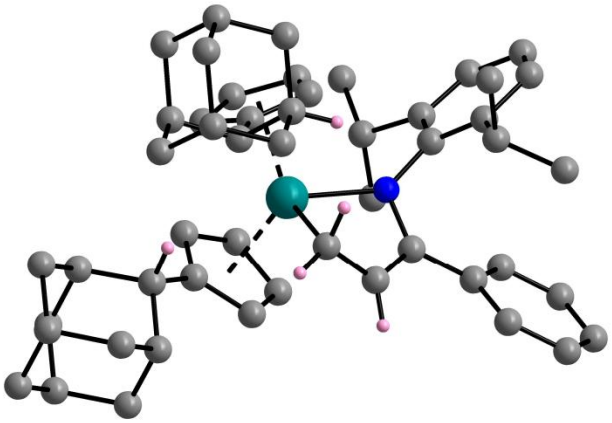

Figure S22: Molecular structure of **2b**.

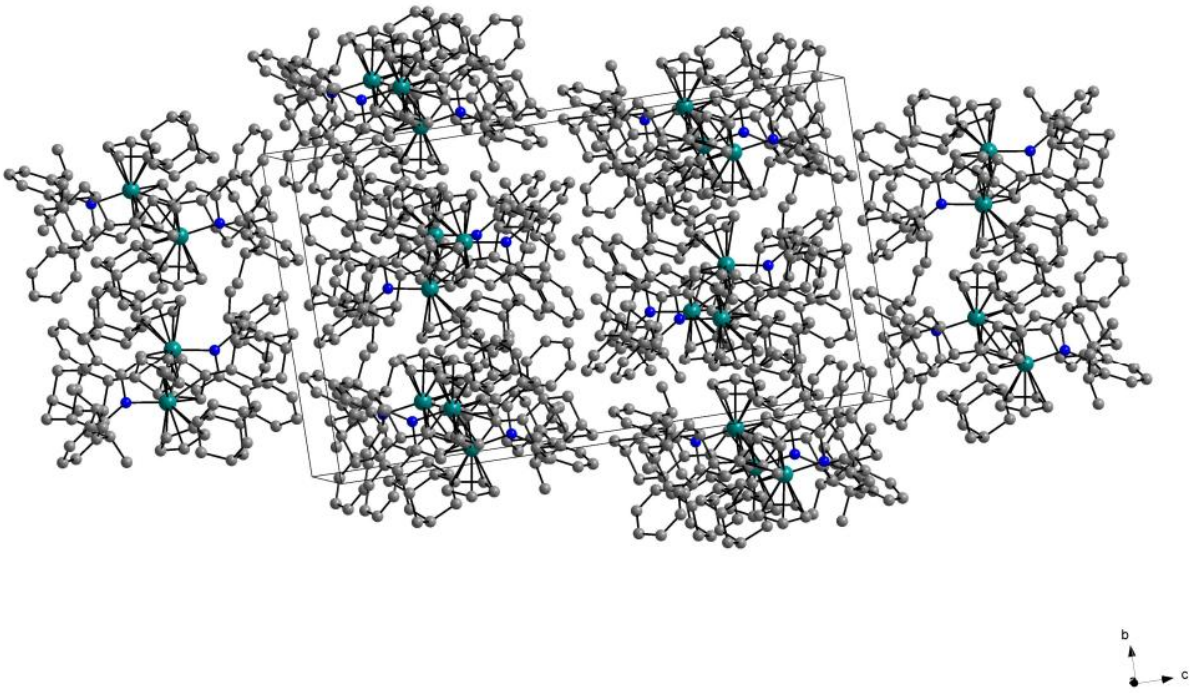

Figure S23: View along the *a* axis showing the packing of molecules in the crystal structure of complex **2b**. Hydrogen atoms have been omitted for clarity.

References

[S1] M. Manßen, S. de Graaff, M.-F. Meyer, M. Schmidtmann, R. Beckhaus, *Organometallics* **2018**, *37*, 4506-4514.

[S2] L. Krause, R. Herbst-Irmer, G. M. Sheldrick, D. Stalke, *J. Appl. Cryst.* **2015**, *48*, 3-10.

[S3] G. M. Sheldrick, *Acta Cryst.* **2008**, *A64*, 112-122.

[S4] G. M. Sheldrick, *Acta Cryst.* **2015**, *C71*, 3-8.

[S5] O. V. Dolomanov, L. J. Bourhis, R. J. Gildea, J. A. K. Howard, H. Puschmann, *Appl. Cryst.* **2009**, *42*, 339-341.